IJISEM
INTERNATIONAL JOURNAL OF INNOVATIONS IN SCIENCE ENGINEERING AND MANAGEMENT

Examine the Effect of Various Fin Shapes in PCM in Solar Energy Storage Unit Using Computational Fluid Dynamics

OPEN ACCESS

Volume: 3

Issue: 3

Month: August

Year: 2024

ISSN: 2583-7117

Published: 07.08.2024

Citation:

Md. Zaid Iqbal[1], Shivendra Singh[2], Dr. B. Suresh[3] "Examine the Effect of Various Fin Shapes in PCM in Solar Energy Storage Unit Using Computational Fluid Dynamics" International Journal of Innovations In Science Engineering And Management, vol. 3, no. 3, 2024, pp. 57–67.

Md. Zaid Iqbal[1], Shivendra Singh[2], Dr. B. Suresh[3]
[1]Research Scholar, Department of Mechanical Engineering, Corporate Institute of Science & Technology, Bhopal
[2]Asst Prof., Department of Mechanical Engineering, Corporate Institute of Science & Technology, Bhopal
[3]Prof. & HOD, Department of Mechanical Engineering, Corporate Institute of Science & Technology, Bhopal.

Abstract
Results from a numerical study of a "latent heat thermal energy storage (LHTES)" vessel's heat storage system are presented in this work. By integrating a new shape of fin into the heat storage process inside a latent heat storage tank, the internal "phase change material" has enhanced heat transfer efficiency. To make sure the numerical model is accurate, we use the experimental data. This study investigates the impact of a variety of architectural designs on the rate of PCM melting and the "temperature distribution" within a "latent heat thermal energy storage (LHTES)" tank. It is also measured how "natural convection" affects the energy storage system. The findings indicate that altering the angle arrangement between fins from 90º (case 1) to 120º (case 2) may lead to a substantial reduction in melting time, namely by 19.6%. To optimize the "energy storage efficiency" in the PCM, it is important to evenly distribute the fins with a set area. This allows for maximum use of both top buoyant convection and lower heat conduction. Case 2 and case 3 have identical fin areas, however their shapes vary. By using fins of varying shapes but with identical surface area, the heat transmission is improved and the rate of melting is reduced by 25.5% and 7.3% compared to case 1 and case 2, respectively. Using different shape and angle orientation of fins in case 4, with lower fin area as compare to remaining all cases. It enhances heat transport and decreases melting duration by 17.6% compared to instance 1, but raises it by 2.4% and 10.5% compared to case 2 and case 3, respectively.

Keyword: Heat transfer fluid, Melting rate, Liquid fraction, Latent heat thermal energy storage, Fins.

INTRODUCTION

The production of energy serves as the primary catalyst for worldwide advancements in many sectors of society, such as the economy and scientific endeavors. Nevertheless, the combination of an economic crisis, volatile oil and gas prices, geopolitical challenges, and an increasing environmental awareness has led to a significant adoption and advancement of renewable energy sources [1]. These sources are clean, globally accessible, and limitless. Furthermore, energy efficiency has emerged as a crucial objective due to its role in achieving energy savings and implementing high-efficiency systems, which are essential for advancing towards a more sustainable and environmentally friendly society. Global energy policy are influenced by this circumstance, both in Western and Eastern nations [2]–[4]

When it comes to the use of energy, the building industry ranks high in industrialised nations. Take the European Union as an example: the construction industry is responsible for about 40% of the region's CO_2 emissions and nearly 40% of its final energy consumption. Most of it may be traced back to rising heating and cooling needs as a result of higher average incomes[5], [6]. It is becoming more and more necessary for non-sustainable buildings to rely on active systems to maintain acceptable levels of internal temperature. In addition, this causes a rise in both energy consumption and the emissions of greenhouse gases [7], [8]. Thus, the cost of running a structure has increased.

Energy efficiency and building sustainability may be greatly advanced by measures such as decreasing cooling load and enhancing energy conservation. More importantly for cutting down on buildings' energy use, however, is the mandated usage of renewable energy sources [9]–[11].

There are primarily two types of applications: passive and active. The former includes more conventional high thermal inertia solutions for buildings, while the latter includes more modern TES units. Materials and architectural components with high thermal inertia are used to create TES, which in turn attenuates thermal oscillations inside the interior space to improve the thermal performance of the structure [12], [13]. When it comes to passive building design, only sensible and latent heat storage are employed [14]. "Thermally Activated Building systems (TABS) or Thermal mass activation (TMA) refers to using the building structure as a TES system through active applications." [15] The method of operation is achieved by coupling a high-heat-capacity building component to a thermal energy supply. These uses make no use of the more exotic forms of thermal storage, such as the photonic or magnetic kind [16]–[18].

Encapsulated "phase change materials (PCMs)" constitute the basis of "thermal energy storage (TES)," which are used to boost the environmental performance of their respective systems by, for the most part, keeping the PCM frozen overnight so that it may be used as a cooling source during the day [19]. As a result, it functions as a cost-free AC by mitigating the effects of the sun's heat throughout the day. "There are two broad categories for the uses of TES components: (1) PCM in ventilation systems for free cooling ventilation, and (2) PCM in PV panels for increased electrical yield due to a decrease in surface temperature increase in comparison to a system without PCMs." [20]–[22]

Miniature "thermal energy storage systems", may use sensible, latent, or thermochemical storage to keep your home comfortably warm or cold. The energy efficiency of HVAC&R systems may be enhanced, and/or the usage of renewable energy can be expanded (via seasonal or daily storage) [23]. "Large-scale thermal energy storage (TES)" systems include both UTES systems that are constructed underground and large-scale water tanks that are built above ground. Solar energy storage for use in DH systems or massive buildings is their primary field of use [24]–[26].

OBJECTIVE

- To study the effect of changing the angle orientation of fin.
- To study the effect of different orientation of fins with constant surface area.
- To study the effect of reducing the fin surface area.
- To study the effect of different shape of fin with constant surface area of fin.

RESEARCH AND METHODOLOGY

Governing equation

Here are the assumptions that the LHTES device uses for its heat transmission and energy preservation processes:

- The buoyancy-driven convection in the molten "phase change material" is characterized by its incompressibility.
- In addition to the liquid density, all other characteristics of the PCM remain unchanged.
- The "phase change process" consists of three phases: solid, transition (mushy), and liquid.
- The density of molten PCM complies with the Boussinesq conditions.
- Volume expansion is not taken into account when the "phase change material" melts.

The following equations may describe the melting phenomenon given these assumptions.

Continuity equation:

$$\frac{\partial u}{\partial x} + \frac{\partial u}{\partial x} = 0$$

Momentum equation:

$$\frac{\partial(\rho u)}{\partial t} + u\frac{\partial(\rho u)}{\partial x} + v\frac{\partial(\rho u)}{\partial y} = \frac{\partial}{\partial x}\left(\mu\frac{\partial u}{\partial x}\right) + \frac{\partial}{\partial y}\left(\mu\frac{\partial u}{\partial y}\right) - \frac{\partial p}{\partial x} + Su$$

$$\frac{\partial(\rho v)}{\partial t} + u\frac{\partial(\rho v)}{\partial x} + v\frac{\partial(\rho v)}{\partial y} = \frac{\partial}{\partial x}\left(\mu\frac{\partial v}{\partial x}\right) + \frac{\partial}{\partial y}\left(\mu\frac{\partial v}{\partial y}\right) - \frac{\partial p}{\partial y} + Sv + \rho_f g\beta(T_f - T_{m_2})$$

Energy equation:

For PCM:

$$\rho_f C_{pf}\frac{\partial T}{\partial t}+\rho_f C_{pf}\left(u\frac{\partial T}{\partial x}+v\frac{\partial T}{\partial y}\right) = \frac{\partial}{\partial x}\left(\lambda\frac{\partial T}{\partial x}\right)+\frac{\partial}{\partial y}\left(\lambda\frac{\partial T}{\partial y}\right)+Se$$

For fin:

$$\rho_{fin}C_{pfin}\frac{\partial T}{\partial t}=\frac{\partial}{\partial x}\left(\lambda\frac{\partial T}{\partial x}\right)+\frac{\partial}{\partial y}\left(\lambda\frac{\partial T}{\partial y}\right)$$

Where S and Se are the source terms expressed by:

$$S=-\frac{(1-f_m)^2}{f_m^3+\xi}C_{mush}$$

$$Se=\rho_f L_f\frac{\partial f_m}{\partial t}$$

The "dynamic viscosity," "specific heat," "coefficient of thermal expansion," "temperature," "thermal conductivity," "pressure," and "density" for the PCM are denoted by the variables μ, C_p, δ, T, λ, p, and ρ, respectively. Velocity is represented by u and v, while the local "liquid (melting) fraction" is denoted by fm. In order to prevent division by zero, a tiny number ξ is used, with the exact value being ξ=10−4. Cmush = 107 represents the mushy coefficient, whereas g stands for the "gravitational acceleration". The "f" stands for the liquid PCM, whereas the "fin" refers to the fin itself.

In order to determine the melting phenomenon and track and quantify the amount of material that has melted, the LHTES device employs the enthalpy-porosity approach. Functions in fm are defined by

$$f_m=\begin{cases}0 & (T\le T_{m1})\\ \dfrac{T-T_{m1}}{T_{m2}-T_{m1}} & (T_{m1}<T<T_{m2})\\ 1 & (T\ge T_{m2})\end{cases}$$

Tm1 and Tm2 are the temperatures at which the PCM transitions from solid to liquid and from liquid to solid, respectively. The soft area is located between the two states.

Latent heat thermal energy storage

Figure 1 is a diagram of the "solar collector system", which includes the phase change tank. The solar receiver takes the sun's rays and concentrates them into usable form. After being heated inside the receiver tube, the "heat transfer fluid (HTF)" is pumped out via the pipes. The purpose of the LHTES tank is to allow heat to be transferred from the Heat passage fluid (HTF) to the phase change material (PCM). Two coaxial tubes make up the LHTES apparatus. Figure 2(a) shows that the "heat transfer fluid" flows through the inner tube, while the phase change material (PCM) fills the outer tube. The inner tube's exterior is covered with gradient fins that are spaced out in a strategic manner. The length of the fin progressively increases as it extends from the base of the fin towards the inner wall of the tube. A two-dimensional system is used to depict the LHTES device since the radial temperature difference is bigger than the axial one, as seen in Figure 2(b). The thermal insulating layer on the LHTES device makes it safe to presume that the boundary wall heat loss is negligible.

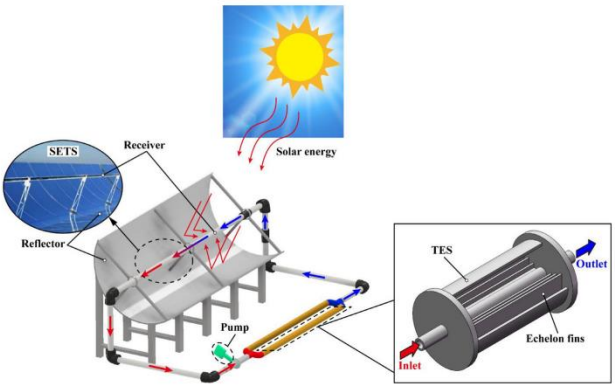

Figure 1 A solar energy-collecting device that includes a heat storage tank.

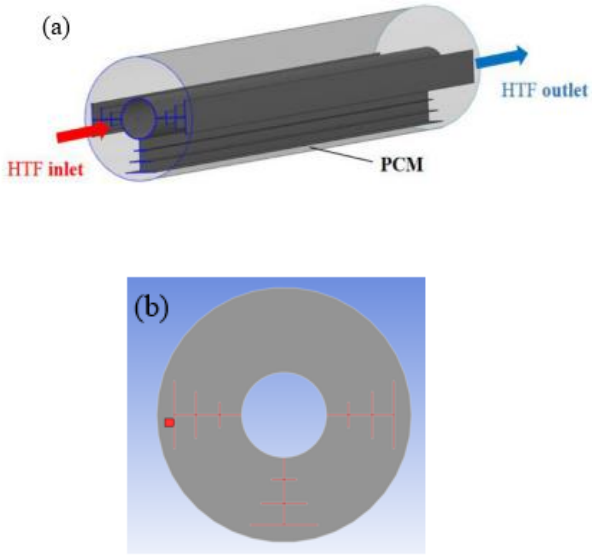

Figure 2 The LHTES tank is shown in both (a) three-dimensional and (b) two-dimensional.

Computational model

Based on the local distribution of fins, the current research employs four configurations of fins in LHTES devices. In case 1, and case 2, fins are same in dimension but different in angular distribution in surface of HTF tube. Fin configure in case 1 is attach to downward at 90º with each other, dimension of the fins and other part illustrate in figure 3. In case 2, fin surface area and dimension of fin branches is same as use in case 1 but the angle between each fins are 120 ºand dimension of the computational model is illustrate in figure 3. In case 3, redesign the fin with different dimension of the branches and angle between each fins is 120º, which is illustrate in figure 3. In this case fin area is increases as compare to case 1 and case 2. In case 4, redesign the fins and angle between each fins is 120º, dimension of the fin is illustrate in figure 3. The table 1 displays the areas of the fins for each case, which are used to improve the heat transfer between the HTF fluid and PCM.

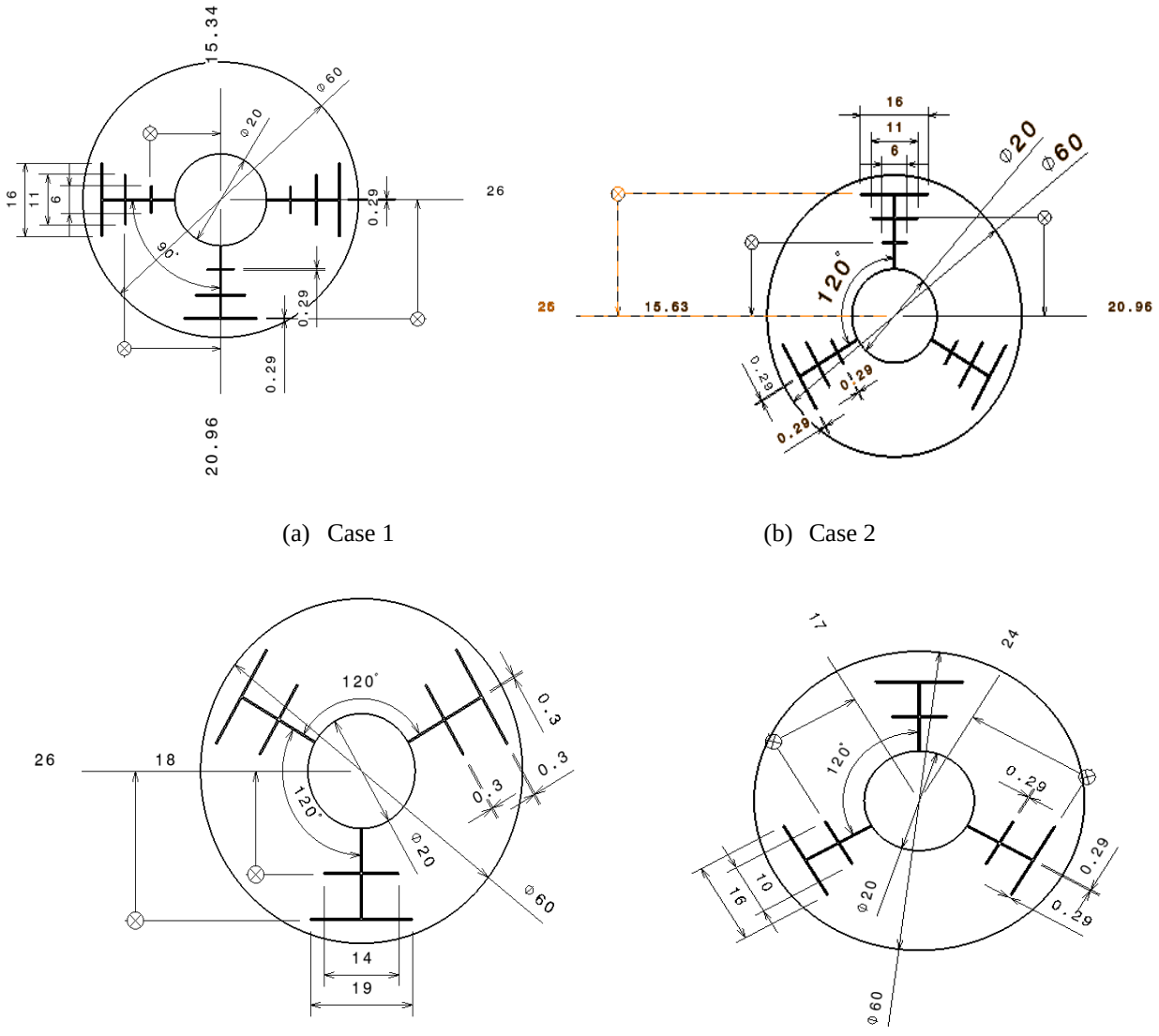

(a) Case 1 (b) Case 2

(c) Case 3 (d) Case 4

Figure 3 Computation model of all Case with dimension

Table 1 Area of the Fin

Cases	Fins area (meter)
Case 1	4.2 E-05
Case 2	4.2 E-05
Case 3	4.36 E-05
Case 4	3.44 E-05

Table 2 Meshing details

Cases	Element	Nodes
Case 1	11657	11785
Case 2	11614	11748
Case 3	11325	11457
Case 4	10284	10425

Mesh generation

Meshing is a method of partitioning computational domains into smaller volumes for the purpose of calculation. The ANSYS Fluent application was used to conduct the meshing procedure. For all the cases of configuration of fins select default meshing method in which element shape is both triangular and quadrilateral. There are two type of element size performed, which is 0.0008 m for PCM domain, and 0.0002 for fin domain. Meshing of all cases for considered configuration of fins illustrate in figure 4 and the detail are mention in table 2.

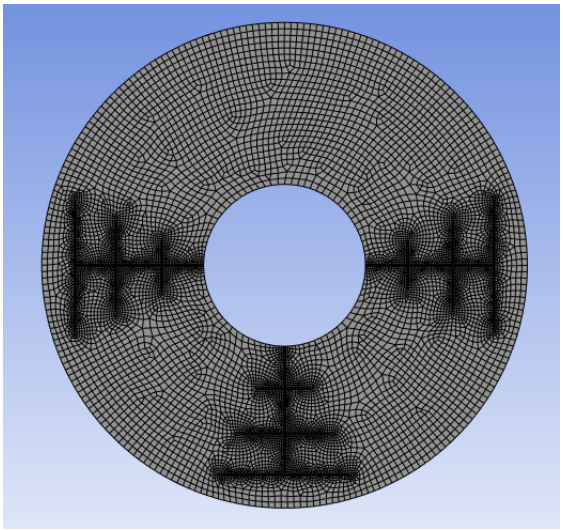

Figure 4 Representative mesh for the computational domain

Numerical method and boundary condition

In order to provide a more streamlined computation model, the beginning conditions and boundary conditions are merged together. The "ANSYS-Fluent 23" program solves the governing equations using the "finite volume technique" (FVM). This procedure discretizes the three governing equations. In the solution technique, pressure-velocity coupling is implemented using the SIMPLE approach. The second-order upwind approach is used for the spatial discretization of the momentum, energy, and pressure equations. For "pressure", "momentum", "energy", and "liquid fraction" selection in the solution control, the corresponding values are 0.3, 0.7, 1, and 0.9. 1e−5, 1e−5, and 1e−6 are the convergence criteria for continuity, velocity, and energy, respectively. Aluminum and Paraffin (RT56) select as HTF tube and PCM material, “thermos-physical properties” of these material show in the table 3. Outer shell body work as adiabatic and HTF tube and fins coupled with constant temperature of 80ºC. When the melting process starts, the "phase change material" is at a temperature of 20ºC.

Table 3 Thermo-physical characteristics of Paraffin and aluminum

Parameters	Units	Paraffin (RT56)	Aluminium
Latent heat (h)	(J/kg)	232,400	-
Melting temperature (T_m)	$(°C)$	55-57	-
Specific heat (C_P)	$(J/kg \cdot K)$	2176	871
Thermal conductivity (λ)	$(W/m \cdot K)$	0.089 (solid/liquid)	202.4
Viscosity (μ)	$(kg/m \cdot s)$	0.00356 (solid/liquid)	-
Thermal expansion coefficient (β)	(K^{-1})	0.00075	-
Density (ρ)	$(kg \cdot m^{-3})$	771.2 (solid/liquid)	2719

MODEL VALIDATION

In the experiment described by (Z. Liu et al., 2023)[27], the LHTES tube's partial computational domain is shown in Figure 3 (a). The "computational domain" for the LHTES tube, which was used to verify the model in this study. Two tubes, 60 mm and 20 mm in diameter, are arranged in a concentric pattern to form the LHTES device. Fin dimension are illustrate in figure 3(a). Aluminium and paraffin (RT56) material use for HTF tube and PCM respectively. The phase change material (PCM) is initially in a solid state at a

constant temperature of 20ºC. The PCM is completely filled inside the aluminum container. Outer shell body work as a adiabatic. For melting the PCM apply constant temperature of 80ºC in HTF tube. Figure 5 depicts the duration required to completely melt the PCM, which is 50 minutes for (Z. Liu et al., 2023)[27] and 51 minutes for the current work.

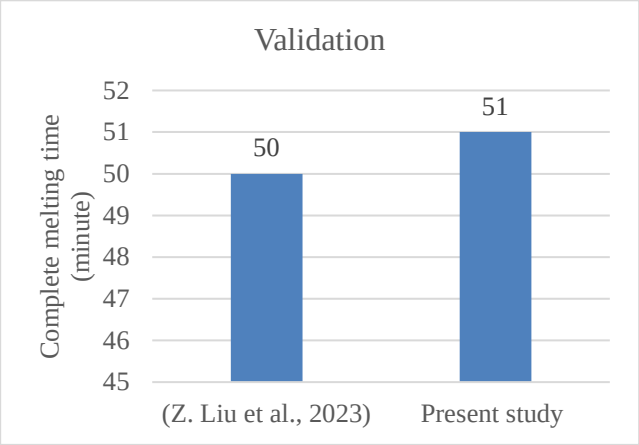

Figure 5 Complete melting time comparison

RESULT AND DISCUSSION

Liquid fraction

Figure 6- 9 Illustrate the melting behavior of PCM in all four cases at 6 different time. In case 1, two fins attach in horizontal and one in vertical down axis. In case 2, equally distribute the angle between each fin, in which two fins are in down side and one is upside of the LHTES device. Case 3, having 3 fins equally distributed angle between each fins with different dimension of the fin. In which one fin downside and other two are in upside of the LHTES device. Case 4, having 3 fins equally distributed angle between each fins with different dimension. In which two are in downside and on in upside. At the completing the 1 minute of melting liquid fraction contour illustrate the PCM start melting around circular HTF tube and slowly moving around fins surface in all four cases. Liquid fraction contour illustrate the after completing the 5 minute of melting PCM melt around the HTF tube and fins and after 10 minutes of melting PCM get 50% melt due to natural convection. After 5 minutes of processing, the PCM will have melted entirely surrounding the fins and HTF tube owing to natural convection, and then it will have melted entirely due to conduction. In all cases, melting process is same at the 10 minutes of melting. Case 1 having a maximum melting rate because of all fin are in downside of the LHTS device. After equally distribution of angle between each fins, illustrate the enhancement in heat transfer.

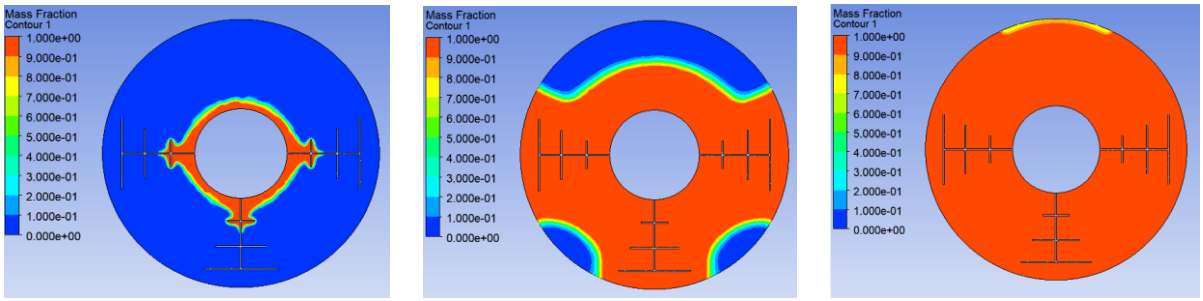

At 1 minute At 20 minute At 51 minute

Figure 6 Liquid fraction contour of case 1

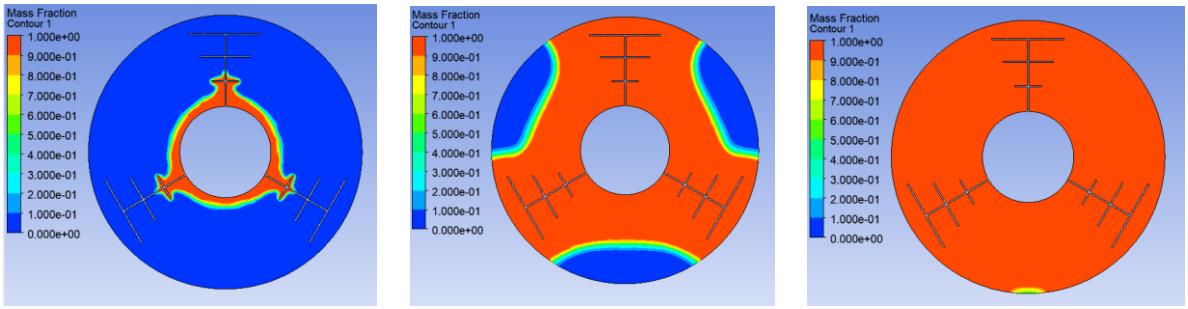

At 1 minute At 20 minute At 41 minute

Figure 7 Liquid fraction contour of case 2

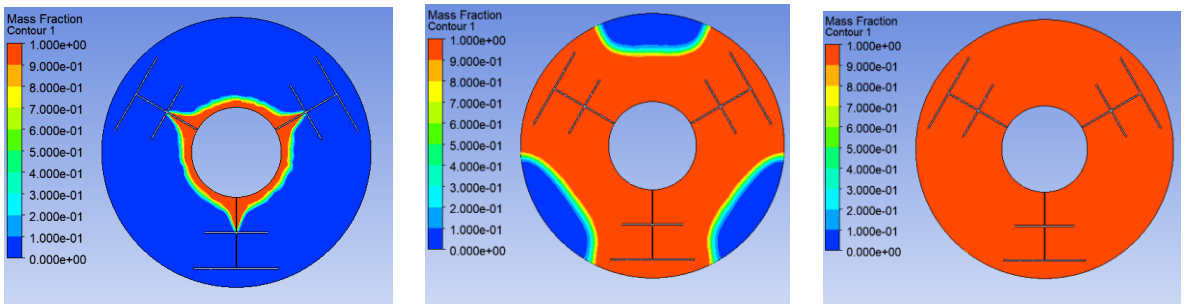

At 1 minute At 20 minute At 38 minute

Figure 8 Liquid fraction contour of case 3

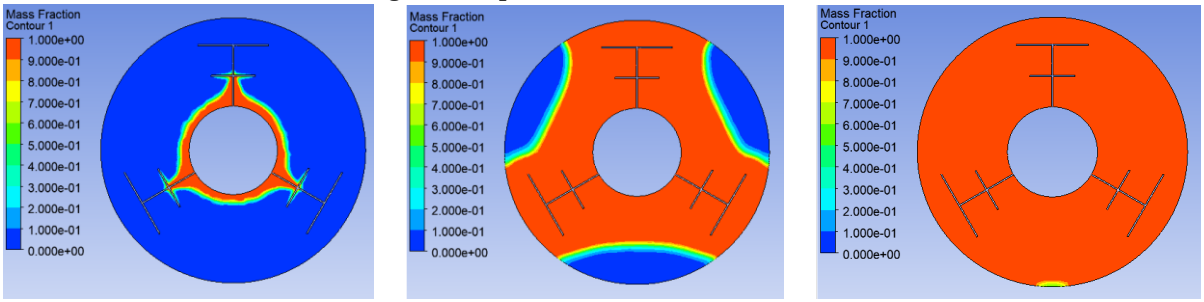

At 1 minute At 20 minute At 42 minute

Figure 9 Liquid fraction contour of case 4

Temperature distribution

Phase change materials (PCMs) possess the potential to undergo physical state transitions within a certain temperature range. Within this document, it is seen that when the “phase change material” is subjected to an increase in temperature reaching its melting point, a transformation from a solid state to a liquid state will take place. During the process of melting, the “phase change material” integrates and retains a substantial quantity of latent heat. The fluctuation in temperature is a crucial indicator for assessing the efficiency of the system. The performance of the various fins is analyzed by examining the temperature diagram (Figure 10-13). The temperature control diagram in Figure 10-13 and the liquid phase fraction contour diagram in Figure 6-9 share the same time period. In one minute, the phase change material (PCM) between the inner tube's surface and the surface of the "heat transfer coefficient" tube will be in direct touch with the heat source, causing the PCM's temperature to begin to rise. The aluminum fin has a higher conductivity than the PCM. Like a tree's branches, the fins allow heat to radiate outward from the inner tube wall's base. Consequently, the PCM around the fin undergoes progressive heating, leading to the transmission of heat to the surrounding PCM. This demonstrates that by adjusting the fins' angle, the heat transmission process may be enhanced, leading to improved energy storage efficiency. The "phase change material" near the fin reaches its melting point after 10 minutes. Case 1, having the low heat transfer rate as compare to other case, due to all fins are place in downside of the LHTES device. Initially, it depends on the process of heat conduction. When a "liquid phase change material" melts, it transports to the melting point and enlarges it. Herein, high temperature area are present in lower side in case 1, and upper side in other cases.

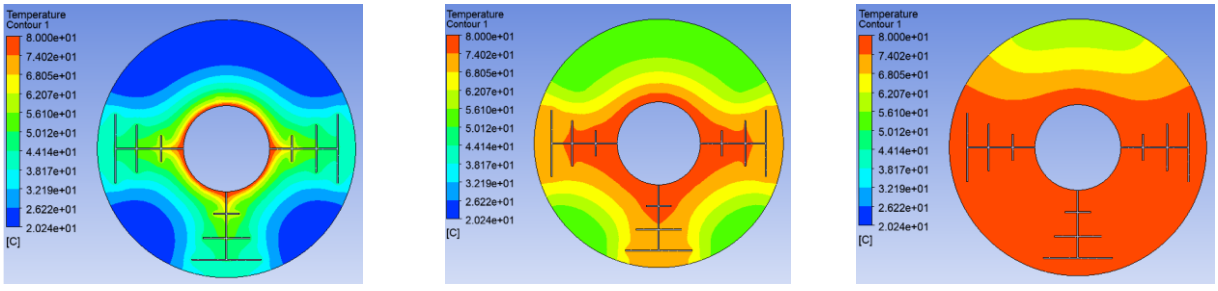

At 1 minute At 20 minute At 51 minute

Figure 10 Temperature distribution contour of case 1

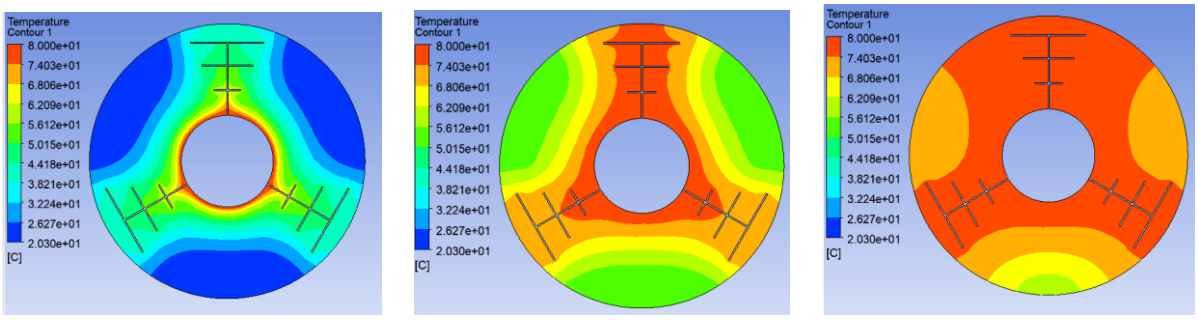

At 1 minute At 20 minute At 41 minute

Figure 11 Temperature distribution contour of case 2

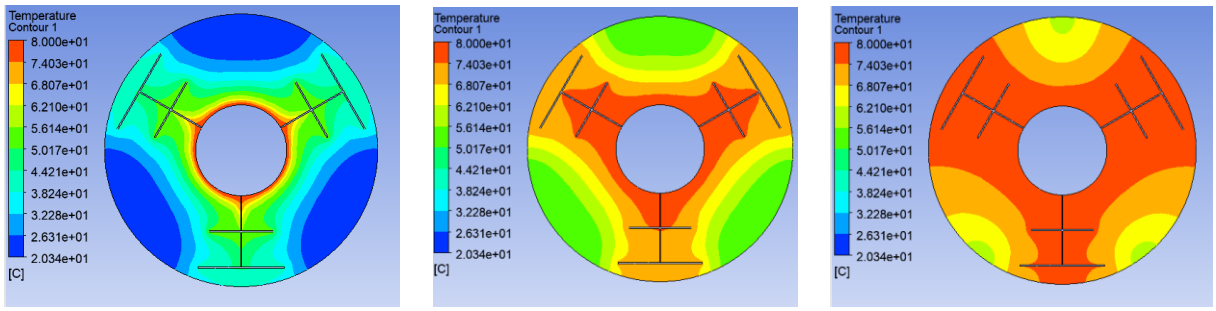

At 1 minute At 20 minute At 38 minute

Figure 12 Temperature distribution contour of case 3

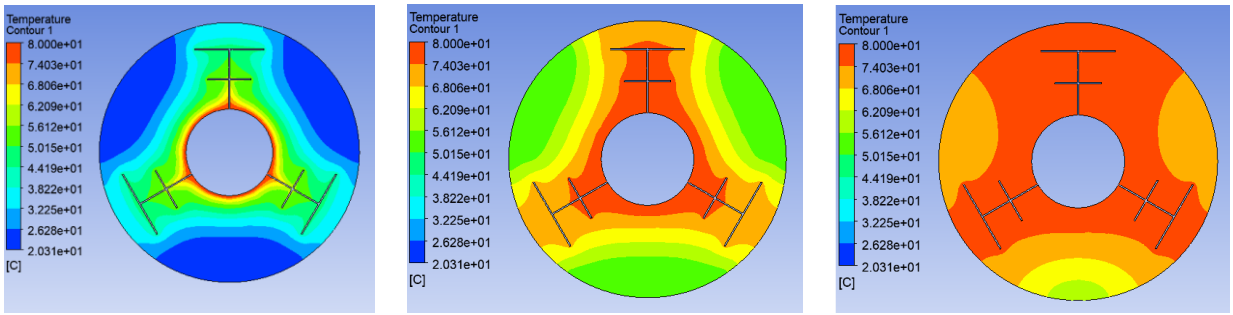

At 1 minute At 20 minute At 42 minute

Figure 13 Temperature distribution contour of case 4

DISCUSSION

Temperature distribution behaviour in all cases are same which is illustrate in figure 16. For melting behaviour of PCM in all cases is same until 10 minute or process after that it increases. Temperature of the PCM start with 20ºC, PCM feel sudden increment under one minute of melting. At the 5 minute of melting temperature is slightly increases due to conduction. PCM temperature riches to 55ºC in 5 minute of melting. After that temperature of PCM get uniformly increases due to natural convection take place, it is illustrate in figure 16. In cases 1, 2, 3, and 4, the final PCM temperatures are 75.38 ºC, 74.48 ºC, 73.83 ºC, and 75.28 ºC, respectively, after the melting process. At the 5 minute of melting liquid fraction is slightly increases due to conduction. After that, it get uniformly behaviour due to natural convection take place. Case 1, having maximum melting time of 51 minute because of all fins are place in lower part of the LHTES device. By equally distributing the angle between each fins decreases the melting time as enhancing the heat transfer. Melting time of case 2, case 3,

and case 3, is 41 minute, 38 minute, and 42 minute respectively. Fin area is same in case1, case2, and case 3 but in case 4, it reduces as compare to other cases.

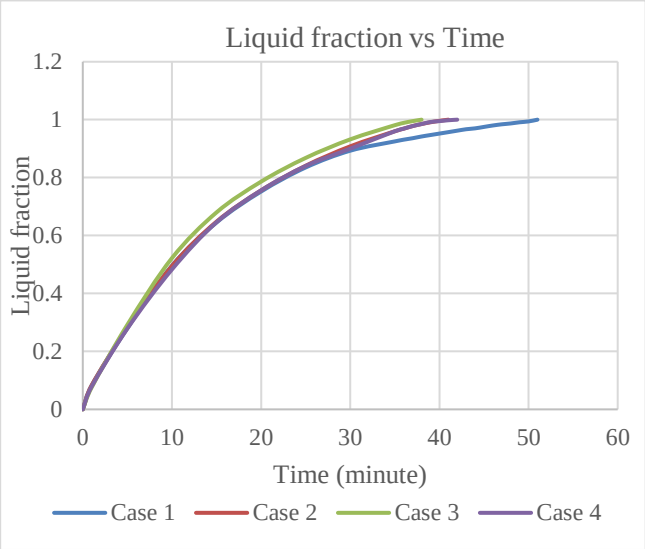

Figure 14 Liquid fraction of PCM with respect to time in all cases

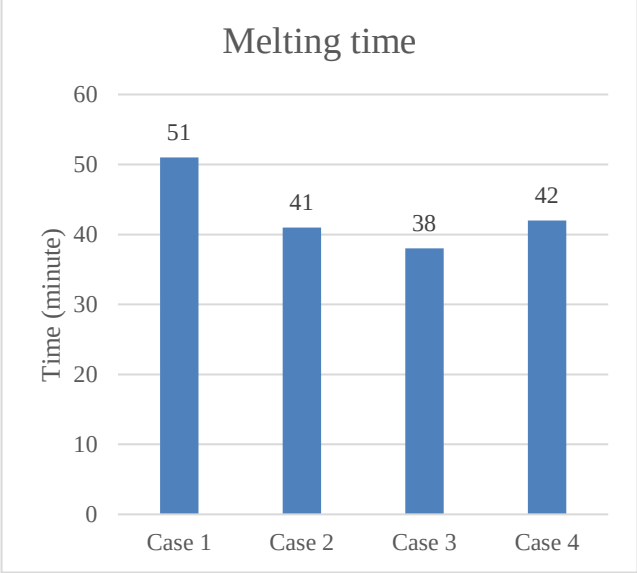

Figure 15 Complete melting time of PCM in all cases

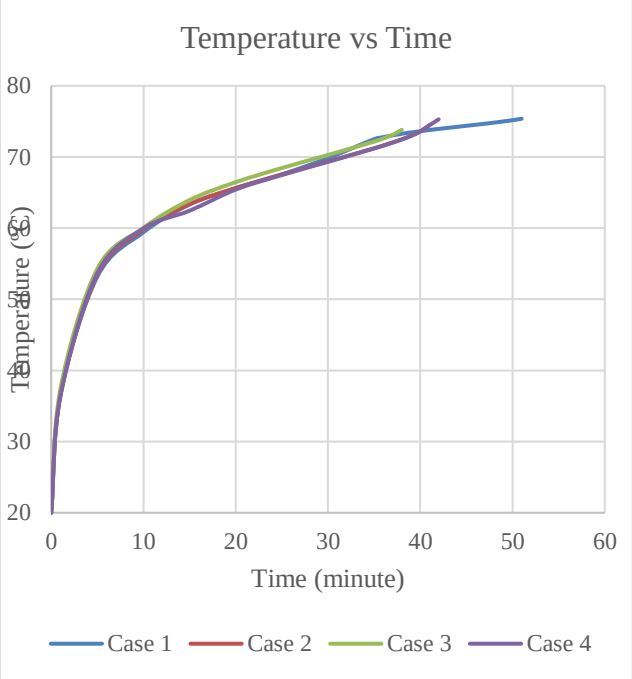

Figure 16 Temperature of PCM with respect to time in all cases

CONCLUSION

An improved sun harvesting system that makes use of a finned LHTES tank is proposed in this study. A unique design has been devised for the form of the gradient fin, with particular emphasis on the layout of its placement. The LHTES tank's gradient fins are arranged at a lower angle, or an angle that is distributed uniformly over all of the fins. The melting point and rate of melting of the "phase change materials" were investigated using verified numerical simulations. Compare the two cases of "phase change material" melting: one in which the fin's surface area is equal to that of the PCM, and another in which the fin's surface area is decreased. The following inferences may be made:

- To maximize the energy storage efficiency in the PCM, it is beneficial to evenly distribute the fins with a set area. This allows for optimal use of both upper buoyant convection and lower heat conduction.
- By replacing the fin angle of 90º (case 1) with 120º (case 2), the heat transmission rate is improved and the melting rate is reduced by 19.6%.
- Case 2 and case 3 possess identical fin areas, although exhibit distinct shapes. An improvement in heat transmission efficiency—a 25.5% decrease in the melting rate relative to case 1 and a 7.3%

decrease in case 2—is achieved by utilizing fins of different shapes with the same surface area.

- Case 4 utilizes fins with varying shapes and angles, and has a smaller fin area compared to the other cases. When compared to case 1, it improves thermal conductivity and shortens melting time. As opposed to case 1, this situation results in a 17.6% reduction in melting time.
- In case 4, the melting time rises by 2.4% compared to case 2, and by 10.5% compared to case 3.

References

[1] M. S. Shafiq, M. M. Khan, and M. Irfan, "Performance enhancement of double-wall-heated rectangular latent thermal energy storage unit through effective design of fins," *Case Stud. Therm. Eng.*, vol. 27, no. August, p. 101339, 2021, doi: 10.1016/j.csite.2021.101339.

[2] K. Hosseinzadeh, M. Alizadeh, and D. D. Ganji, "Solidification process of hybrid nano-enhanced phase change material in a LHTESS with tree-like branching fin in the presence of thermal radiation," *J. Mol. Liq.*, vol. 275, pp. 909–925, 2019, doi: 10.1016/j.molliq.2018.11.109.

[3] A. Mahdavi, M. A. Erfani Moghaddam, and A. Mahmoudi, "Simultaneous charging and discharging of multi-tube heat storage systems using copper fins and Cu nanoparticles," *Case Stud. Therm. Eng.*, vol. 27, no. August, p. 101343, 2021, doi: 10.1016/j.csite.2021.101343.

[4] J. Wołoszyn, K. Szopa, and G. Czerwiński, "Enhanced heat transfer in a PCM shell-and-tube thermal energy storage system," *Appl. Therm. Eng.*, vol. 196, p. 117332, 2021, doi: 10.1016/j.applthermaleng.2021.117332.

[5] R. Qaiser, M. M. Khan, L. A. Khan, and M. Irfan, "Melting performance enhancement of PCM based thermal energy storage system using multiple tubes and modified shell designs," *J. Energy Storage*, vol. 33, no. August 2020, p. 102161, 2021, doi: 10.1016/j.est.2020.102161.

[6] L. A. Khan, M. M. Khan, H. F. Ahmed, M. Irfan, D. Brabazon, and I. U. Ahad, "Dominant roles of eccentricity, fin design, and nanoparticles in performance enhancement of latent thermal energy storage unit," *J. Energy Storage*, vol. 43, no. February, p. 103181, 2021, doi: 10.1016/j.est.2021.103181.

[7] V. Kumar, S. Singh, S. Engineering, V. Kumar, and S. Singh, "' Heat Transfer Enhancement in Triplex Tube Latent Heat Energy Storage System Using Tree Fins and Variation on Branch Angle ,'" pp. 16–25, 2024.

[8] S. Singh, "A Review on Nano-PCM based Thermal Energy Storage for Various Applications," pp. 85–88, 2023.

[9] L. Zheng, W. Zhang, and F. Liang, "A review about phase change material cold storage system applied to solarpowered air-conditioning system," *Adv. Mech. Eng.*, vol. 9, no. 6, pp. 1–20, 2017, doi: 10.1177/1687814017705844.

[10] M. Sheikholeslami, M. Jafaryar, Z. Said, A. I. Alsabery, H. Babazadeh, and A. Shafee, "Modification for helical turbulator to augment heat transfer behavior of nanomaterial via numerical approach," *Appl. Therm. Eng.*, vol. 182, p. 115935, 2021, doi: 10.1016/j.applthermaleng.2020.115935.

[11] B. G. Abreha, P. Mahanta, and G. Trivedi, "Thermal performance evaluation of multi-tube cylindrical LHS system," *Appl. Therm. Eng.*, vol. 179, no. June, p. 115743, 2020, doi: 10.1016/j.applthermaleng.2020.115743.

[12] L. A. Khan and M. M. Khan, "Role of orientation of fins in performance enhancement of a latent thermal energy storage unit," *Appl. Therm. Eng.*, vol. 175, no. December 2019, p. 115408, 2020, doi: 10.1016/j.applthermaleng.2020.115408.

[13] S. Bandaru, "A Study on Latent Heat Thermal Energy Storage System with Tree-like Branching Fin," pp. 27–37, 2023.

[14] M. Vivekananthan and V. A. Amirtham, "Characterisation and thermophysical properties of graphene nanoparticles dispersed erythritol PCM for medium temperature thermal energy storage applications," *Thermochim. Acta*, vol. 676, pp. 94–103, 2019, doi: 10.1016/j.tca.2019.03.037.

[15] J. Vogel and A. Thess, "Validation of a numerical model with a benchmark experiment for melting governed by natural convection in latent thermal

energy storage," *Appl. Therm. Eng.*, vol. 148, pp. 147–159, 2019, doi: 10.1016/j.applthermaleng.2018.11.032.

[16] N. Kousha, M. Rahimi, R. Pakrouh, and R. Bahrampoury, "Experimental investigation of phase change in a multitube heat exchanger," *J. Energy Storage*, vol. 23, no. February, pp. 292–304, 2019, doi: 10.1016/j.est.2019.03.024.

[17] Z. Li *et al.*, "Solidification process through a solar energy storage enclosure using various sizes of Al2O3 nanoparticles," *J. Mol. Liq.*, vol. 275, pp. 941–954, 2019, doi: 10.1016/j.molliq.2018.11.129.

[18] V. Kumar and S. Singh, "CFD analysis of Rectangular Thermal Energy Storage System using Polyethylene Glycol 1500 as a PCM with fins," pp. 62–71, 2023.

[19] M. M. Joybari, S. Seddegh, X. Wang, and F. Haghighat, "Experimental investigation of multiple tube heat transfer enhancement in a vertical cylindrical latent heat thermal energy storage system," *Renew. Energy*, vol. 140, pp. 234–244, 2019, doi: 10.1016/j.renene.2019.03.037.

[20] M. Faghani, M. J. Hosseini, and R. Bahrampoury, "Numerical simulation of melting between two elliptical cylinders," *Alexandria Eng. J.*, vol. 57, no. 2, pp. 577–586, 2018, doi: 10.1016/j.aej.2017.02.003.

[21] L. Begum, M. Hasan, and G. H. Vatistas, "Energy storage by melting commercial change phase materials in hexagonal-shaped heat exchangers," *J. Thermophys. Heat Transf.*, vol. 32, no. 4, pp. 1013–1030, 2018, doi: 10.2514/1.T5341.

[22] A. Raj, S. Singh, and B. Suresh, "Enhanced the solidification of the phase change material in the horizontal latent heat thermal energy storage by using rectangular plate and circular disc plate fins by using CFD," pp. 89–96, 2023.

[23] L. Roccamena, M. El Mankibi, and N. Stathopoulos, "Development and validation of the numerical model of an innovative PCM based thermal storage system," *J. Energy Storage*, vol. 24, no. April, p. 100740, 2019, doi: 10.1016/j.est.2019.04.014.

[24] N. Fadaei, A. Kasaeian, A. Akbarzadeh, and S. H. Hashemabadi, "Experimental investigation of solar chimney with phase change material (PCM)," *Renew. Energy*, vol. 123, pp. 26–35, 2018, doi: 10.1016/j.renene.2018.01.122.

[25] A. E. Kabeel and M. Abdelgaied, "Solar energy assisted desiccant air conditioning system with PCM as a thermal storage medium," *Renew. Energy*, vol. 122, pp. 632–642, 2018, doi: 10.1016/j.renene.2018.02.020.

[26] A. M. Abdulateef, S. Mat, K. Sopian, J. Abdulateef, and A. A. Gitan, "Experimental and computational study of melting phase-change material in a triplex tube heat exchanger with longitudinal/triangular fins," *Sol. Energy*, vol. 155, pp. 142–153, 2017, doi: 10.1016/j.solener.2017.06.024.

[27] Z. Liu *et al.*, "Effect of phase change heat storage tank with gradient fin structure on solar energy storage: A numerical study," *Int. J. Heat Mass Transf.*, vol. 215, p. 124384, 2023, doi: 10.1016/j.ijheatmasstransfer.2023.124384.